Measurement of Local Sodium Ion Levels near Micelle Surfaces with Fluorescent Photoinduced-Electron-Transfer Sensors

Published in:
Angewandte Chemie International Edition

Document Version:
Peer reviewed version

Queen's University Belfast - Research Portal:
Link to publication record in Queen's University Belfast Research Portal

Measurement of Local Sodium Ion Levels near Micellar Surfaces with Fluorescent PET (Photoinduced Electron Transfer) Sensors

Seiichi Uchiyama,*[a,b] Eiko Fukatsu,[b] Gareth D. McClean,[a] and A. Prasanna de Silva*[a]

[a]   Dr. S. Uchiyama, Dr. G. D. McClean, Prof. A. P. de Silva
        School of Chemistry and Chemical Engineering
        Queen's University
        Belfast BT9 5AG (Northern Ireland)
        E-mail: a.desilva@qub.ac.uk
[b]   Dr. S. Uchiyama, E. Fukatsu
        Graduate School of Pharmaceutical Sciences
        The University of Tokyo
        7-3-1 Hongo Bunkyo-ku Tokyo 113-0033 (Japan)
        E-mail: seiichi@mol.f.u-tokyo.ac.jp

        Supporting information for this article is given via a link at the end of the document.

Abstract: Na^+ near membranes controls our nerve signals, besides several other crucial bioprocesses. We demonstrate that fluorescent PET (photoinduced electron transfer) sensor molecules target Na^+ in nanospaces near micellar membranes with excellent discrimination against H^+. They find that Na^+ near anionic micelles is concentrated by factors of upto 160. Sensor molecules which are not held tight to the micelle surface find a Na^+ amplification factor of 8 only. These findings are strengthened by the employment of control compounds whose PET processes are permanently 'on' or permanently 'off'.

Biological membranes organize living matter in cells, create a fluid three-dimensional matrix and allow for the controlled transport of solutes.[1] Many biologically important processes are membrane-mediated, yet surprisingly little is known about both reaction schemes and more fundamentally complex nano-environments where reactions occur. For instance, the gradient of Na^+ concentration across biological membranes is involved in transport of molecules into cells, pH homeostasis, and signal transmission in nerve systems,[2] and is regulated by proteins such as Na^+/K^+-ATPase,[3] Na^+/H^+ antiporter,[4] and voltage-gated Na^+ channel.[5] Accurate measurement of local Na^+ levels near model membranes such as aqueous micellar surfaces[6] requires sensors with excellent selectivity against ubiquitous H^+, very few of which are available.[7] Although membrane-bounded H^+ have been measured with fluorescent sensors,[8] only a few larger ions (but not Na^+) have been measured near micelle surfaces and even then only with sensors whose fluorescence output is influenced by H^+.[9] The related field of ion-driven, micelle-bound logic systems has very few examples.[10] We now measure local Na^+ levels near a micellar surface with designed PET (photoinduced electron transfer) sensors[11] for the first time.

Figure 1 indicates the chemical structures of fluorescent PET sensors (**1a**-**1d** and **4a**-**4b**) used in this study. These sensors are designed based on the 'fluorophore-spacer-receptor' concept.[12] The benzo-15-crown-5 structure is chosen as a receptor due to its well-known binding properties towards Na^+ (c.f. log β_{Na^+} value of benzo-15-crown-5 is 0.4 in water[13]). Importantly, the binding ability of the receptor with Na^+ is not affected by environmental pH change because it does not contain a pH-sensitive structure (e.g. amino group). Anthracene is adopted as a fluorophore in **1a**-**1d** due to its high hydrophobicity to be positioned inside micelles.[14] In addition, the anthracene structure participates in a non-radiative PET process when outfitted with an electron withdrawing substituent in R when the benzo-15-crown-5 unit is Na^+-free.[15] Otherwise

it emits strong fluorescence. Benzofurazan is also adopted as a fluorophore of the sensors (in **4a**-**4b**). Along with the above characteristics described for anthracene, the benzofurazan structure has the remarkable feature that the maximum emission wavelength is dramatically shifted to shorter values in a hydrophobic environment.[8c,16] In both cases (**1a**-**1d** and **4a**-**4b**), a short methylene spacer is used for efficient fluorescence switching based on the PET mechanism and an anchor substituent is varied to change the local position of the sensor within the membrane-bounded nanoenvironment.

2a-**2d** and **5a**-**5b** are critically important control compounds during studies of nanoenvironments, which always involve PET due to the dimethoxybenzene moiety being unable to bind Na^+ (i.e. always fluorescence 'off'). Thus the fluorescence properties of **2a**-**2d** and **5a**-**5b** can be influenced only by the salt-induced environmental change of micelles (e.g. polarity change). **3** and **6** are additional control compounds that are free from PET (i.e. always fluorescence 'on').[17]

In the present study, a variety of anionic, cationic, and neutral micelles are investigated as they all introduce different nanoenvironments. Figure 2 shows the chemical structures of the surfactants used in this study. All of the micelles possess less polar regions than the surrounding aqueous environment but the presence of negatively charged, positively charged, and neutral head groups have a great influence over how the micelles interact with the surrounding environment. For instance, cationic Na^+ is expected to be concentrated near the negatively charged head group of the micelles by electrostatic attraction.

Na^+ concentration near micellar surfaces is evaluated by studying the fluorescence properties of the sensors as a function of bulk Na^+ concentration. This method, previously applied to H^+,[8] is applied to Na^+ for the first time. Interactions between the fluorescent sensors (or control compounds) and the surfactants in micellar solutions could be confirmed by a dramatic increase in their solubility compared to those in water. Also, the hypsochromic shift of maximum emission wavelengths of the benzofurazan compounds (**4a**, **4b**, **5a**, and **5b**) in micellar solution (Table 1) indicates that these sensors and control compounds are in a hydrophobic environment, i.e. close to or inside the micelles. Representative fluorescence behaviours of the sensors and the control compounds in micellar solutions are shown in Figures 3 and 4. The most important result is that the fluorescence switching 'on' of the sensors with increasing [Na^+] is observed only in TMADS solution (Figure 4, see also Figure S1 and Table 2). This behaviour disappears when the control compounds are used instead, indicating that the fluorescence switching 'on' of the sensors is due to Na^+ binding rather than due to any change in micellar nanoenvironment (e.g. local polarity) caused by salt effects.[18] In contrast to TMADS solution, the fluorescence switching of the sensors by Na^+ is not seen in CTAC, Triton X-100 or OG solutions. Although it was reported that the binding ability of benzo-15-crown-5 towards Na^+ increased in less polar media,[13] this effect is not observed even in Triton X-100 micelles that create the most hydrophobic environment for the sensors in the present study (see maximum emission wavelength in Table 1). This is because ions avoid less polar membranes, preferring adjacent aqueous regions instead.[8c] Thus we conclude that Na^+ is concentrated near TMADS micelles because of electrostatic attraction to the negatively charged sulfonate group of the surfactant.

The local Na^+ concentration near TMADS micelles is determined by the $\Delta\log\beta_{Na^+}$ value ($\log\beta_{Na^+}$ in TMADS solution $-\log\beta_{Na^+}$ in water) of the sensors,[19] parallel to the ΔpK_a method previously applied to micelle-bounded H^+.[8a,20] Table 2 summarized the $\log\beta_{Na^+}$ values of the sensors in micellar solution that are obtained using the equation,

$$\log[(I_{max}-I)/(I-I_{min})] = pNa - \log\beta_{Na^+}$$

where I, I_{max}, and I_{min} are the observed fluorescence intensity at a fixed wavelength, the corresponding maximum and minimum, respectively. Given the modular behaviour of fluorescent PET sensors,[12] the $\log\beta_{Na^+}$ value in water would be 0.4 (the value for benzo-15-crown-5[13]). On that basis, the $\Delta\log\beta_{Na^+}$ values are calculated to be 2.0 (for **1a** and **1b**), 2.1 (**1c**), 0.9 (**1d**), and 2.2 (**4a** and **4b**). Therefore the local Na^+ concentration observed by the sensors near the TMADS micellar surface is 7.9-158 ($=10^{0.9}-10^{2.2}$) times higher than what is present in bulk water. The range of micelle-bounded Na^+ concentrations found by the sensors can be ascribed to their different locations in the micellar system.[8c] In the Na^+ gradient created by TMADS micelles, the neutral sensor **1d** would be located closer to bulk water whereas the other cationic sensors are distributed closer to the micelle surface by ion paring with the head group. If the position of the sensors are controlled more extensively,[8c] our method would construct the Na^+ gradient near the micelle in more detail. Development of new receptors showing stronger binding ability to Na^+ in aqueous media is also important because fluorescent sensors having such receptors will be able to determine Na^+ concentration even near neutral and cationic micelles where Na^+ is repelled in comparison to bulk water by dielectric effects and/or an electrostatic repulsion.

In summary, a series of new fluorescent PET sensors measure local Na^+ concentrations which are electrostatically concentrated in nanospaces[21] near anionic micelles for the first time. Similar experiments in nanospaces near more biorelevant membranes such as vesicles and liposomes will be our next step. Another important step for future biological use would be to improve Na^+/K^+ selectivity of these sensors while preserving pH-independence. The available diversity of fluorescent PET sensor components for various targets[11,12] will also allow us to measure other important ions in biological nanoenvironments in a similar manner.

[1] a) M. S. Bretscher, *Sci. Am.* **1985**, *253(4)*, 86-90; b) *Molecular Biology of the Cell*, 6th ed. (Eds.: B. Alberts, A. Johnson, J. Lewis, D. Morgan, M. Raff, K. Roberts, P. Walter), Garland Science, New York, **2015**, pp. 597-640.

[2] F. M. Harold, *The Vital Force-A Study of Bioenergetics*, Freeman, New York, **1986**, pp. 318-332.

[3] a) J. C. Skou, *Biochim. Biophys. Acta* **1957**, *23*, 394-401; b) J. H. Kaplan, *Annu. Rev. Biochem.* **2002**, *71*, 511-535.

[4] K. A. Williams, *Nature* **2000**, *403*, 112-115.

[5] J. Payandeh, T. Scheuer, N. Zheng, W. A. Catterall, *Nature* **2011**, *475*, 353-358.

[6] J. H. Fendler, *Membrane Mimetic Chemistry*, Wiley, New York, **1982**.

[7] A. P. de Silva, K. R. A. S. Sandanayake, *J. Chem. Soc., Chem. Commun.* **1989**, 1183-1185.

[8] a) M. S. Fernández, P. Fromherz, *J. Phys. Chem.* **1977**, *81*, 1755-1761; b) R. A. Bissell, A. J. Bryan. A. P. de Silva, C. P. McCoy, *J. Chem. Soc., Chem. Commun.* **1994**, 405-407; c) S. Uchiyama, K. Iwai, A. P. de Silva, *Angew. Chem. Int. Ed.* **2008**, *47*, 4667-4669; *Angew. Chem.* **2008**, *120*, 4745-4747.

[9] a) S. Bhattacharya, A. Gulyani, *Chem. Commun.* **2003**, 1158-1159; b) K. Niikura, E. V. Anslyn, *J. Org. Chem.* **2003**, *68*, 10156-10157; c) Y. Nakahara, T. Kida, Y. Nakatsuji, M. Akashi, *Org. Biomol. Chem.* **2005**, *3*, 1787-1794; d) J. B. Wang, X. H. Qian, J. H. Qian, Y. F. Xu, *Chem. Eur. J.* **2007**, *13*, 7543-7552; e) H. Tian, J. Qian, H. Bai, Q. Sun, L. Zhang, W. Zhang, *Anal. Chim. Acta* **2013**, *768*, 136-142; f) N. Kumari, N. Dey, S. Jha, S. Bhattacharya, *ACS Appl. Mater. Interfaces* **2013**, *5*, 2438-2445.

[10] a) S. Uchiyama, G. D. McClean, K. Iwai, A. P. de Silva, *J. Am. Chem. Soc.* **2005**, *127*, 8920-8921; b) Y. Diaz-Fernandez, F. Foti, C. Mangano, P. Pallavicini, S. Patroni, A. Perez-Gramatges, S. Rodriguez-Calvo, *Chem. Eur. J.* **2006**, *12*, 921-930; c) A. P. de Silva, C. M. Dobbin, T. P. Vance, B. Wannalerse, *Chem. Commun.* **2009**, 1386-1389; d) P. Pallavicini, Y. A. Diaz-Fernandez, L. Pasotti, *Coord. Chem. Rev.* **2009**, *253*, 2226-2240.

[11] a) A. P. de Silva, H. Q. N. Gunaratne, T. Gunnlaugsson, A. J. M. Huxley, C. P. McCoy, J. T. Rademacher, T. E. Rice, *Chem. Rev.* **1997**, *97*, 1515-1566; b) L. Prodi, *New J. Chem.* **2005**, *29*, 20-31; c) J. F. Callan, A. P. de Silva, D. C. Magri, *Tetrahedron* **2005**, *61*, 8551-8588; d) J. Chan, S. C. Dodani, C. J. Chang, *Nat. Chem.* **2012**, *4*, 973-984; e) Y. Yang, Q. Zhao, W. Feng, F. Li, *Chem. Rev.* **2013**, *113*, 182-270.

[12] a) A. P. de Silva, T. S. Moody, G. D. Wright, *Analyst* **2009**, *134*, 2385-2393; b) A. P. de Silva, *J. Phys. Chem. Lett.* **2011**, *2*, 2865-2871; c) B. Daly, J. Ling, A. P. de Silva, *Chem. Soc. Rev.* **2015**, *44*, 4203-4211.

[13] R. M. Izatt, R. E. Terry, D. P. Nelson, Y. Chan, D. J. Eatough, J. S. Bradshaw, L. D. Hansen, J. J. Christensen, *J. Am. Chem. Soc.* **1976**, *98*, 7626-7630.

[14] C. D. Tran, T. A. Van Fleet, *Anal. Chem.* **1988**, *60*, 2478-2482.

[15] A. P. de Silva, K. R. A. S. Sandanayake, *Tetrahedron Lett.* **1991**, *32*, 421-424.

[16] a) T. Oe, M. Morita, T. Toyo'oka, *Anal. Sci.* **1999**, *15*, 1021-1023; a) C. Gota, S. Uchiyama, T. Yoshihara, S. Tobita, T. Ohwada, *J. Phys. Chem. B* **2008**, *112*, 2829-2836.

[17] Double control experiments of this kind are rare. In the related but different field of fluorescent pH sensors, reference compounds displaying pH-independent high PET rates and pH-independent low PET rates are known to bracket the pH-dependent behaviour of the sensor itself. See: A. P. de Silva, S. A. de Silva, A. S. Dissanayake, K. R. A. S. Sandanayake, *J. Chem. Soc., Chem. Commun.* **1989**, 1054-1056.

[18] Y. Yue, J. Wang, M. Dai, *Langmuir* **2000**, *16*, 6114-6117.

[19] For a detailed description of Δlog β_{Na^+}, see Supporting Information.

[20] S. Basili, T. D. Giacco, F. Elisei, R. Germani, *Org. Biomol. Chem.* **2014**, *12*, 6677-6683.

[21] K. Sumaru, H. Matsuoka, H. Yamaoka, G. D. Wignall, *Phys. Rev. E* **1996**, *53*, 1744-1752.

[22] P. Mukerjee, K. J. Mysels, P. Kapauan, *J. Phys. Chem.* **1967**, *71*, 4166-4175.

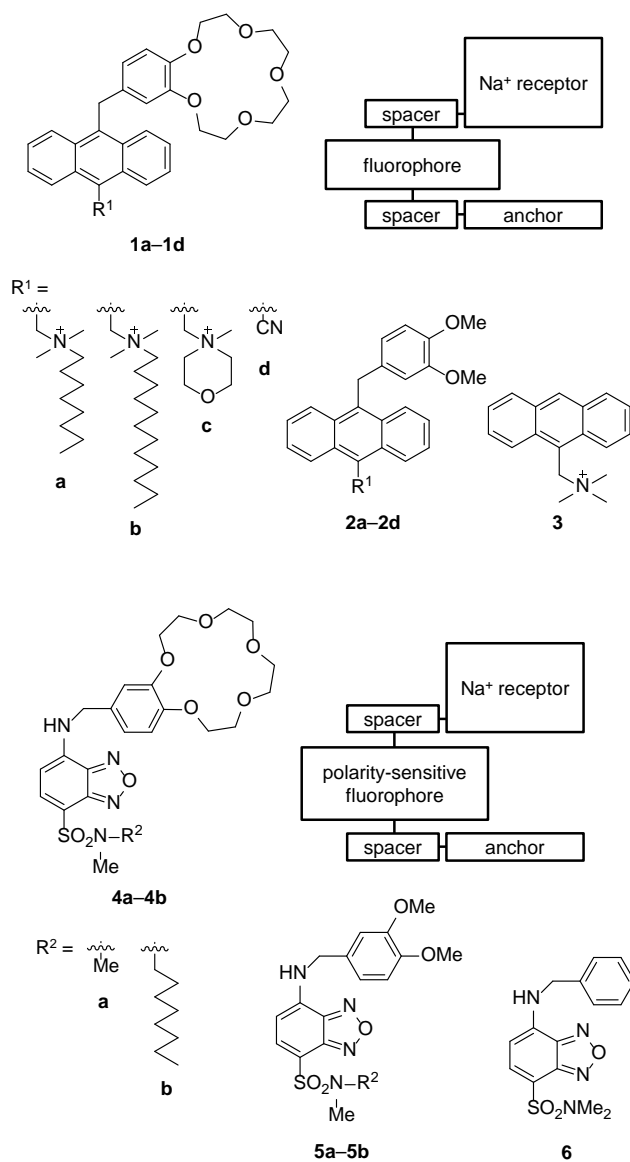[23] R. von Wandruszka, *Crit. Rev. Anal. Chem.* **1992**, *23*, 187-215.

R^1 =

a **b** **c** **d**

1a–1d

2a–2d **3**

R^2 =

a **b**

4a–4b

5a–5b **6**

Figure 1. Chemical structures of fluorescent sensors for Na$^+$ (**1a-1d** and **4a-4b**) and control compounds (**2a-2d**, **3**, **5a-5b**, and **6**) used in this study. Counter ion is Br$^-$ for **1a-1c** and **2a-2c**, and Cl$^-$ for **3**.
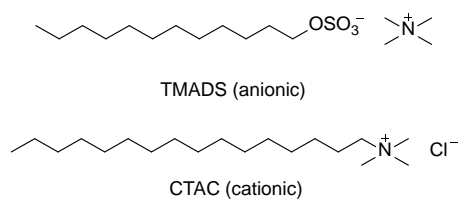
TMADS (anionic)

CTAC (cationic)

Figure 2. Chemical structures of the surfactants used in this study. Critical micelle concentration (cmc): 5.5 mM for TMADS (tetramethylammonium dodecyl sulfate[22]), 1.4 mM for CTAC (cetyltrimethylammonium chloride[23]), 0.24 mM for Triton X-100,[23] and 25 mM for OG (octyl β-D-glucopyranoside[23]).

a) **1a** + TMADS

ex. 376 nm

pNa
1.0
1.6
2.2
2.8
4.0
∞

b) **2a** + TMADS

ex. 377 nm

pNa
1.0
1.6
2.2
2.8
4.0
∞

c) **4a** + TMADS

ex. 430 nm

pNa
1.0
2.2
2.5
2.8
3.1
∞

d) **5a** + TMADS

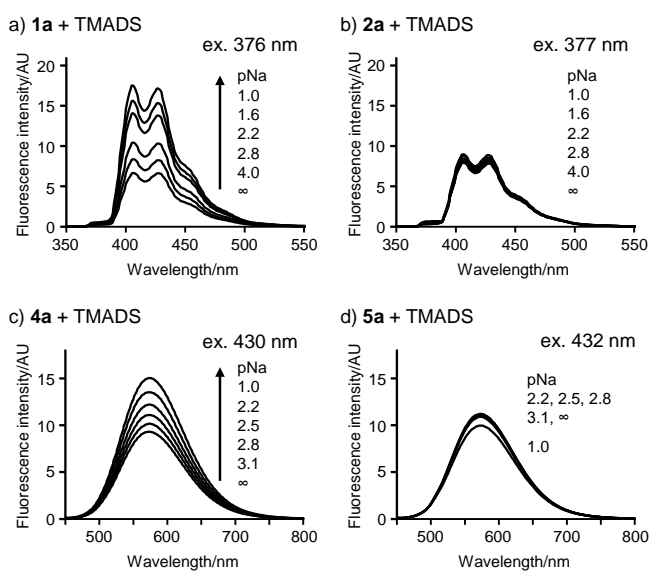ex. 432 nm

pNa
2.2, 2.5, 2.8
3.1, ∞

1.0

Figure 3. Representative fluorescence spectra with a variation in Na+ concentration (pNa). a) **1a**, b) **2a**, c) **4a**, and **5a** (10 μM each) in TMADS solution (20 mM). pNa refers to the total in micellar solution and is varied by adding NaCl. Excitation wavelength (ex.) is indicated in each panel.
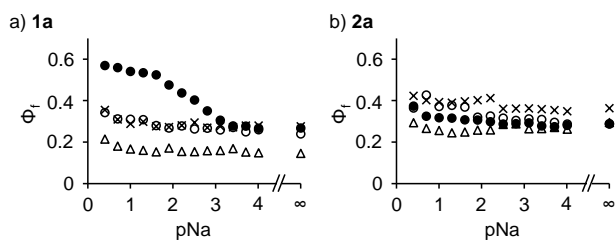
a) **1a**

b) **2a**

Figure 4. Fluorescence quantum yield (Φ_f)-pNa diagrams obtained for a) **1a**, b) **2a**, c) **4a**, and d) **5a** (10 μM) in TMADS (20 mM, closed circle), CTAC (5 mM, open circle), Triton X-100 (0.52 mM, triangle), and OG (34 mM, cross) solutions. pNa refers to the total in micellar solution and is varied by adding NaCl

Table 1. Maximum emission wavelengths of **4a**, **4b**, **5a**, and **5b**.

Solution	Wavelength [nm][a]			
	4a	**4b**	**5a**	**5b**
TMADS (20 mM)	573	573	573	572
CTAC (5 mM)	573	574	573	573
Triton X-100 (0.52 mM)	546	541	563	558
OG (34 mM)	575	563	573	564
water	594	ND[b]	595	ND[b]

[a] Excited at a maximum absorption wavelength. At 25 °C. [b] Could not be determined because of low solubility.

Table 2. Fluorescence properties of the sensors and control compounds in TMADS solution.

Compound	$\Phi_{f.high[Na^+]}$ [a]	$\Phi_{f.low[Na^+]}$ [b]	FE[c]	$\log \beta_{Na^+}$
Anthracene				
1a	0.54	0.27	2.0	2.41 ± 0.18
2a	0.32	0.29		
1b	0.66	0.24	2.7	2.35 ± 0.02
2b	0.17	0.17		
1c	0.81	0.34	2.4	2.50 ± 0.04
2c	0.43	0.35		
1d	0.045	0.0056	8.1	1.26 ± 0.15
2d	0.010	0.0092		
3	0.81	0.78		
Benzofurazan				
4a	0.045	0.028	1.6	2.57 ± 0.02
5a	0.025	0.029		
4b	0.057	0.038	1.5	2.56 ± 0.03
5b	0.031	0.039		
6	0.040	0.047		

[a] [Na$^+$] in solution is 0.1 M. [b] [Na$^+$] in solution is 0 M. [c] Fluorescence enhancement factor ($\Phi_{f.high[Na^+]}$ / $\Phi_{f.low[Na^+]}$).